are approximately in the same plane. The dihedral angle between planes of Cu(1)O(1)Cu(3) and Cu(1)O(2)Cu(3) is 21.8°. This plane is nearly perpendicular to the plane of N(2)O(1)Cu(2)-Cl(2)Cl(3); dihedral angle ≈ 80°. Since compound **2** has three different copper(II) centers and three different Cu–Cu distances, it is a complex system regarding magnetic interactions. Investigation of magnetic properties of this complex is underway.

Cu(II) complexes with mono(amino alcohol) ligands have been known to form[9] dimers or a dimer–dimer linked by weak intermolecular Cu–O bonds. Trimeric species with amino alcohol ligands were previously unknown. The formation of **2** demonstrated that (a) dmap ligand is able to bind to more than two metal centers and (b) compound **1** is an useful precursor for the synthesis of multinuclear Cu compounds. Heterometallic compounds with the dmap ligand using **1** as precursor are currently under investigation in our laboratory.

Acknowledgment. We thank the University of Windsor for financial support for this work.

Supplementary Material Available: Tables S1–S5, listing crystallographic data, H atom parameters, and anisotropic temperature factors for **1** and **2**, and Figures S8 and S9, showing the structures of a disordered toluene molecule in **1** and a CH_2Cl_2 molecule in **2** (9 pages); Tables S6 and S7, listing observed and calculated structure factors for **1** and **2** (27 pages). Ordering information is given on any current masthead page.

Contribution from the Laboratoire de Chimie Inorganique, URA No. 420, Université de Paris-Sud, 91405 Orsay, France, Laboratoire de Physique du Solide, URA No. 002, Université de Paris-Sud, 91405 Orsay, France, and Service National des Champs Intenses, UPR No. 5021, CNRS, 38042 Grenoble, France

Ferromagnetically Coupled $Gd^{III}Cu^{II}$ Molecular Material

Olivier Guillou,[1a] Pierre Bergerat,[1a] Olivier Kahn,*[,1a] Evangelos Bakalbassis,[1a] Kamal Boubekeur,[1b] Patrick Batail,*[,1b] and Maurice Guillot[1c]

Received June 5, 1991

The compound $Gd_2(ox)[Cu(pba)]_3[Cu(H_2O)_5]\cdot 20H_2O$ (**1**), where ox stands for oxalato and pba for 1,3-propylenebis(oxamato), has been synthesized. **1** crystallizes in the monoclinic system, space group $C2/m$. The lattice parameters are a = 21.186 (7) Å, b = 21.098 (2) Å, c = 15.079 (1) Å, and β = 92.06 (2)°, with Z = 4. The crystal structure consists of layers of double-sheet polymers separated by water molecules. A puckered ladderlike arrangement of Gd[Cu(pba)] units forms a two-dimensional honeycomb pattern connected by oxalato groups. Discrete $[Cu(H_2O)_5]^{2+}$ entities are interspersed in the gap between the layers. The temperature dependence of the zero-field magnetic susceptibility down to 1.3 K and the field dependence of the magnetization in both the low-field regime (below 200 G) and the high-field regime (up to 20 T) have been investigated. The magnetic data are consistent with a rather strong spin correlation within the lattice and reveal that the Gd(III)–Cu(II) interaction through the oxamato bridge is ferromagnetic in spite of the large Gd···Cu separations (between 5.693 (1) and 5.739 (1) Å).

Introduction

In the last three years, we[2,3] and Gatteschi, Rey, et al.[4] have synthesized several molecular-based compounds exhibiting a spontaneous magnetization below a critical temperature T_c by assembling ferrimagnetic chains $[AB]_n$ within the crystal lattice in a ferromagnetic fashion. Two of the requirements of this approach are the following: (i) The local spins S_A and S_B of the nearest-neighbor magnetic centers along the chain must be as different as possible, and the antiferromagnetic interaction between them as large as possible. If so, the distance along which the spins S_A are oriented in an upward fashion and the neighboring spins S_B in a downward fashion (or correlation length between $|S_A-S_B|$ units) is important even at relatively high temperature. Up to now, we have used A = Mn(II) and B = Cu(II) ions, with $S_{Mn} = {}^5/_2$ and $S_{Cu} = {}^1/_2$, and bisbidentate-conjugated bridges which possess a remarkable ability to transmit rather strong antiferromagnetic interactions between magnetic centers far apart from each other.[5] (ii) The overall interchain interaction must be ferromagnetic and also as large as possible. Thus, the one-dimensional character is an obvious limitation to obtain relatively high ordering temperatures. In our case, the ferromagnetic interchain interaction has been realized by imposing Mn···Cu instead of Mn···Mn and Cu···Cu as shortest interchain separations along one of the directions perpendicular to the chain axis. The spin structure is then as follows with all the S_{Mn} local spins aligned along the same direction:[6]

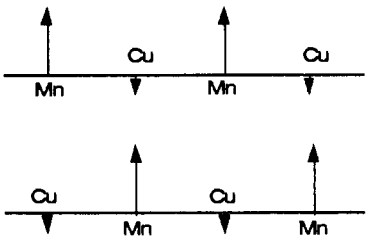

All the copper(II) precursors used until now were divalent anions. One of them is $[Cu(pba)]^{2-}$, pba standing for 1,3-propylenebis(oxamato),[7] shown as follows:

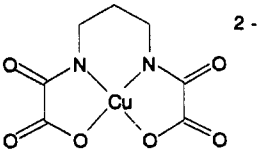

The reaction of $[Cu(pba)]^{2-}$ with a divalent metal ion M(II) in a solvent S affords a one-dimensional compound of formula $MCu(pba)S_n$.[7,8] If $[Cu(pba)]^{2-}$ reacts with a trivalent metal ion M(III), one can expect to obtain a two- or three-dimensional compound of formula $M_2[Cu(pba)]_3S_n$. Increasing the dimensionality is one way to favor bulk magnetic properties. Moreover, if Mn(II) is replaced by Gd(III) with the local spin $S_{Gd} = {}^7/_2$, the spin difference $|S_A-S_B|$ is maximized. In this paper, we report on our first molecular-based compound involving Gd(III) and Cu(II) ions, of formula $Gd_2(ox)[Cu(pba)]_3Cu(H_2O)_5\cdot 20H_2O$ (**1**), where ox stands for oxalato and arises from the hydrolysis of a Cu(pba) group during the reaction. We will successively describe the crystal structure of this compound and its magnetic properties.

(1) (a) Laboratoire de Chimie Inorganique, Orsay. (b) Laboratoire de Physique du Solide, Orsay. (c) Service National des Champs Intenses, Grenoble.
(2) Kahn, O.; Pei, Y.; Verdaguer, M.; Renard, J. P.; Sletten, J. *J. Am. Chem. Soc.* **1988**, *110*, 782.
(3) Nakatani, K.; Carriat, J. Y.; Journaux, Y.; Kahn, O.; Lloret, F.; Renard, J. P.; Pei, Y.; Sletten, J.; Verdaguer, M. *J. Am. Chem. Soc.* **1989**, *111*, 5739.
(4) Caneschi, A.; Gatteschi, D.; Sessoli, R.; Rey, P. *Acc. Chem. Res.* **1989**, *22*, 392.
(5) Kahn, O. *Angew. Chem., Int. Ed. Engl.* **1985**, *24*, 834.
(6) Kahn, O. *Struct. Bonding (Berlin)* **1987**, *68*, 89.
(7) Pei, Y.; Verdaguer, M.; Kahn, O.; Sletten, J.; Renard, J. P. *Inorg. Chem.* **1987**, *26*, 138.
(8) Von Koningsbruggen, P.; Kahn, O.; Nakatani, K.; Pei, Y.; Renard, J. P.; Drillon, M.; Legoll, P. *Inorg. Chem.* **1990**, *29*, 3325.

0020-1669/92/1331-0110$03.00/0

Table I. Crystallographic Data for $Gd_2[Cu(pba)]_3Cu(H_2O)_5 \cdot 20H_2O$

molecular formula	$C_{23}H_{68}Gd_2Cu_4O_{47}N_6$	Z	4
fw	1749.47	T	297 K
space group	$C2/m$	λ	0.71073 Å
a	21.186 (7) Å	d(calc)	1.726 g cm^3
b	21.098 (2) Å	μ	32.94 cm^{-1}
c	15.079 (1) Å	R^a	5.2%
β	92.06 (2)°	$R_w{}^a$	8.2%
V	6735.9 Å^3		

[a] R and R_w are defined through $R = \sum(|F_o| - |F_c|)/\sum|F_o|$ and $R_w = [\sum w(|F_o| - |F_c|)^2/\sum F_o^2]^{1/2}$ with $w = 4F_o^2/\sigma^2(F_o^2)$.

Table II. Positional Parameters and Their Estimated Standard Deviations for $Gd_2[Cu(pba)]_3Cu(H_2O)_5 \cdot 20H_2O$

atom	x	y	z
Gd	0.24095 (2)	0.15001 (2)	0.35286 (3)
Cu1	0.48967 (6)	0.25788 (6)	0.3780 (1)
Cu2	0.250	0.250	0.000
O1	0.2543 (3)	0.0530 (3)	0.4328 (5)
O2	0.2266 (4)	0.0537 (4)	0.2613 (5)
O3	0.3537 (3)	0.1321 (3)	0.3888 (5)
O4	0.3021 (3)	0.2474 (3)	0.3658 (6)
O5	0.3047 (4)	0.1616 (4)	0.2196 (5)
O6	0.1826 (4)	0.1888 (4)	0.2251 (6)
O7	0.1319 (3)	0.1196 (3)	0.3773 (5)
O8	0.1741 (3)	0.2386 (3)	0.3954 (6)
O9	0.2504 (4)	0.1644 (4)	0.5145 (5)
O11	0.0756 (3)	0.2745 (3)	0.3983 (6)
O12	0.4506 (3)	0.1740 (4)	0.3928 (6)
O13	0.4975 (8)	0.2376 (9)	0.220 (1)
N11	0.0300 (4)	0.1607 (4)	0.3763 (7)
N12	0.4040 (4)	0.2884 (4)	0.3725 (7)
O21	0.3068 (5)	0.2071 (7)	0.0847 (7)
O22	0.1874 (5)	0.2317 (7)	0.0860 (7)
O23	0.281 (2)	0.367 (1)	0.082 (2)
C1	0.2488 (6)	0.000	0.394 (1)
C2	0.2318 (7)	0.000	0.296 (1)
C11	0.3908 (4)	0.1774 (5)	0.3857 (7)
C12	0.3621 (4)	0.2445 (5)	0.3732 (7)
C13	0.1151 (5)	0.2310 (5)	0.3912 (7)
C14	0.0913 (4)	0.1634 (5)	0.3800 (7)
C15	0.3849 (5)	0.3551 (5)	0.360 (1)
C16	0.4354 (6)	0.3938 (6)	0.321 (1)
C17	−0.0020 (5)	0.0986 (5)	0.361 (1)
C21	0.2109 (5)	0.2045 (6)	0.1563 (9)
C22	0.2811 (6)	0.1888 (6)	0.1562 (9)
C23	0.373 (2)	0.199 (2)	0.073 (3)
C24	0.402 (5)	0.248 (4)	0.038 (6)
C25	0.123 (2)	0.255 (2)	0.076 (3)
Cu3	0.4592 (3)	0.000	0.5797 (5)
Cu4	0.5820 (3)	0.000	0.3786 (6)
O31	0.516 (3)	0.063 (3)	0.305 (4)
O32	0.419 (3)	0.000	0.386 (4)
O33	0.500	0.076 (2)	0.500
O41	0.392 (2)	0.000	0.459 (3)
O42	0.369 (2)	0.095 (2)	0.594 (2)
O43	0.498 (3)	0.070 (4)	0.411 (4)
OW1	0.294 (2)	0.500	0.391 (2)
OW2	0.725 (1)	0.153 (1)	0.249 (2)
OW3	0.8876 (7)	0.000	0.523 (1)
OW4	0.403 (2)	0.078 (2)	0.196 (2)
OW5	0.095 (1)	0.074 (2)	0.161 (2)
OW6	0.233 (2)	−0.054 (2)	0.061 (3)
OW7	0.191 (3)	0.000	0.805 (3)
OW8	−0.003 (3)	0.143 (2)	0.086 (3)

Experimental Section

Synthesis. The sodium salt of the Cu(II) precursor $Na_2[Cu(pba)] \cdot 6H_2O$ is synthesized as previously described.[7,9] Large blue platelike single crystals of **1** were obtained by slow diffusion in a H-shaped tube at room temperature of equimolecular (2.5×10^{-4} mol) aqueous solutions of $Na_2[Cu(pba)] \cdot 6H_2O$ and $GdCl_3 \cdot 6H_2O$ within ca. 2 months.

Crystallographic Data Collection and Structure Determination. The crystals proved to be stable in contact with their mother liquor only. They were found particularly fragile, breaking very easily into successive thinner plates, a striking manifestation of the layered character of the structure. Therefore, they had to be handled with extreme care. The data collection crystal was mounted in a glass capillary tube filled with water. The data collection details are summarized in Table I. Preliminary oscillation and Weissenberg photographs indicated monoclinic symmetry. Systematic absences, (hkl) reflections for $h + k$ odd, indicate that the crystal belongs to one of the three possible space groups $C2$, Cm, and $C2/m$. The latter was chosen on the basis of intensity statistics and successful refinements. The structure was solved by direct methods and refined by full-matrix least-squares techniques.[10] The Cu(pba) group between the strands is located on a center of symmetry, and atoms O21, O22, O23, C23, C24, and C25 are subsequently disordered. Note that the sites for O21 and O22 are in fact, in this disorder model, admixtures of nitrogen and oxygen atoms. The site occupation factors of the two conformations are properly refined to 50% each. Likewise, two $[Cu(H_2O)_5]^{2+}$ moities were located in the vicinity of the mirror plane and introduced as disordered units. The site occupation factors of their individual atoms, Cu3, Cu4, O31, O32, O33, O41, O42, and O43, were refined to convergence to 50%. Finally, a thermogravimetry analysis of single crystals of the data collection batch indicated the presence of 25 water molecules per formula unit, of which 23 were identified on successive Fourier maps and found to remained stable along isotropic least-square refinements. No attempt was made of introducing any of the 68 hydrogen atoms in the refinements. This, as well as the observed disorder and high thermal motion of all atoms, might account for the discrepancy observed between the R and R_w values. The positional parameters are given in Table II.

Magnetic Susceptibility Measurements. These were carried out with two instruments, namely, (i) an ac mutual inductance bridge working down to 1.3 K and (ii) a Mêtronique Ingêniêrie SQUID magnetometer working down to 1.5 K. This magnetometer can be used in low field (a few gauss) as well as in high field (up to 8 T).

Magnetization Measurements. The low-field magnetization measurements were carried out with the SQUID magnetometer described above. The high-field measurements were performed at the Service National des Champs Intenses by means of a fluxmetric method. The sample was displaced within a constant magnetic field between compensated pick-up coils connected in series opposition. The integrated signal of the induced voltage was proportional to M. The continuous magnetic field up to 20 T was produced by a water-cooled Bitter magnet. The calibration and the sensitivity of the apparatus were previously described in detail.[11]

Table III. Bond Lengths in Gadolinium and Copper Coordination Spheres and Intermetallic Distances (Å)[a]

Gd–O1	2.388 (5)	Gd–Gd[b]	6.1239 (7)
Gd–O2	2.469 (6)	Gd–Gd[c]	6.3362 (7)
Gd–O3	2.457 (5)	Gd–Gd[d]	11.4020 (3)
Gd–O4	2.434 (5)	Gd–Gd[e]	11.4599 (8)
Gd–O5	2.476 (6)	Gd–Cu1[f]	5.7387 (9)
Gd–O6	2.391 (6)	Gd–Cu1[g]	5.6935 (9)
Gd–O7	2.439 (5)	Gd–Cu1[b]	6.7566 (11)
Gd–O8	2.447 (5)	Gd–Cu1[h]	7.2361 (11)
Gd–O9	2.454 (6)	Gd–Cu2[f]	5.2799 (4)
Cu1–O11	1.956 (5)	Gd–Cu3[f]	6.4675 (51)
Cu1–O12	1.972 (6)	Gd–Cu4[i]	6.2659 (51)
Cu1–O13	2.43 (1)	Cu1–Cu1[h]	3.6847 (25)
Cu1–N11	1.921 (6)	Cu1–Cu3[i]	5.5846 (16)
Cu1–N12	1.925 (6)	Cu1–Cu4[f]	5.7867 (23)
Cu2–O21	1.942 (8)		
Cu2–O22	1.930 (9)		
Cu2–O23	2.82 (3)		

[a] Numbers in parentheses are estimated standard deviations in the least significant digits. [b] $-x + 1/2, -y + 1/2, -z + 1$. [c] $x, -y, z$. [d] $x + 1/2, -y + 1/2, z$. [e] $-x + 1/2, -y + 1/2, -z$. [f] x, y, z. [g] $x - 1/2, -y + 1/2, z$. [h] $-x + 1, y, -z + 1$. [i] $-x + 1, -y, -z + 1$.

A Unique Layered Structure

The major structural features are exemplified in Figure 1. The coordinations of the Gd(III) and Cu(II) ions as well as the atom labeling are given in Figure 2. A stereoscopic representation of the unit cell contents is given in Figure 3. Table III contains

(9) Nonoyama, K.; Ojima, H.; Nonoyama, M. *Inorg. Chim. Acta* **1976**, *20*, 127.

(10) Frenz, B. A. Enraf-Nonius SDP-Plus Structure Determination Package. Enraf-Nonius, Delft, The Netherlands, 1985.

(11) Picoche, J. C.; Guillot, M.; Marchand, A. *Physica B* **1989**, *155*, 407.

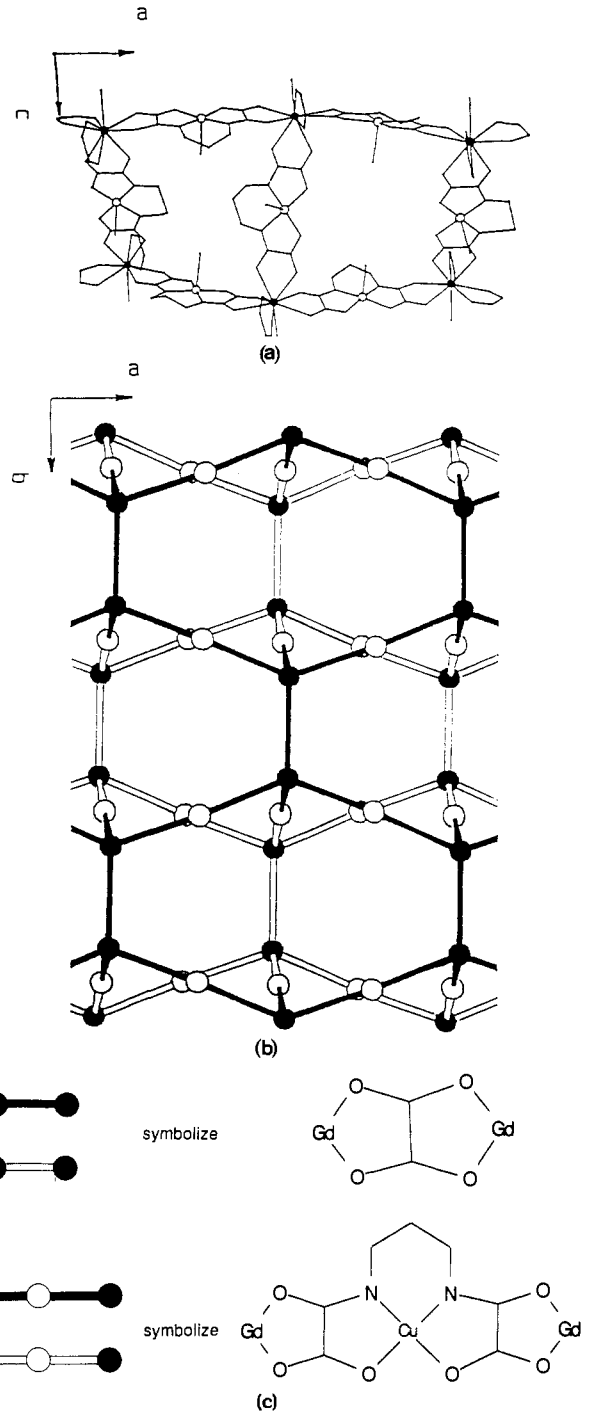

Figure 1. (a) Perspective ORTEP view down the *b* axis of a fraction of a mixed-metal ladder. The Cu atoms (white circles) are essentially coplanar. The puckering pattern is such that the Gd atoms (black circles) alternate above and below the Cu mean plane. (b) Schematic representation of how four such ladders fit together along the transverse *b* direction. This view emphasizes the honeycomb pattern of Gd_6 rings. The solid (open) lines symbolize linkages within the upper (lower) layer, as exemplified in (c).

the bond lengths in the Gd and Cu coordination spheres and the intermetallic distances, and Table IV the bond angles around the metal atoms.

The whole structure has a pronounced two-dimensional character and can be viewed as a succession along the *c*-axis direction of layers of double-sheet coordination polymers filled in by water molecules and separated by discrete $Cu(H_2O)_5$ units. Inside the layers, the metal atoms are arranged in parallel double strands. These mixed-metal atom strands are held together by Cu(pba) units bridging the Gd(III) ions of the individual chains. Thus, a puckered ladderlike arrangement developing along the *a*-axis

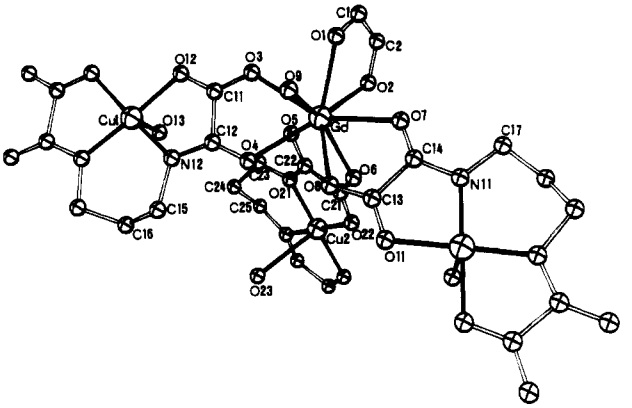

Figure 2. ORTEP view of the a truncated sequence of coordination polyhedra. The labeling of the atoms of the asymmetric unit is indicated.

Table IV. Bond Angles around the Metal Atoms and Intermetallic Angles (deg)[a]

O1–Gd–O2	65.4 (2)	O7–Gd–O8	66.4 (2)
O1–Gd–O3	70.2 (2)	O7–Gd–O9	85.6 (2)
O1–Gd–O4	129.3 (2)	O8–Gd–O9	70.8 (2)
O1–Gd–O5	115.8 (2)	O11–Cu1–O12	93.4 (2)
O1–Gd–O6	138.4 (2)	O11–Cu1–O13	89.6 (4)
O1–Gd–O7	78.0 (2)	O11–Cu1–N11	84.5 (2)
O1–Gd–O8	125.6 (2)	O11–Cu1–N12	173.4 (3)
O1–Gd–O9	66.6 (2)	O12–Cu1–O13	89.8 (4)
O2–Gd–O3	95.3 (2)	O12–Cu1–N11	174.2 (3)
O2–Gd–O4	142.6 (2)	O12–Cu1–N12	84.6 (3)
O2–Gd–O5	71.8 (2)	O13–Cu1–N11	95.6 (4)
O2–Gd–O6	77.6 (2)	O13–Cu1–N12	96.8 (4)
O2–Gd–O7	76.8 (2)	N11–Cu1–N12	96.8 (3)
O2–Gd–O8	135.7 (2)	O21–Cu2–O21	180.(0)
O2–Gd–O9	131.3 (2)	O21–Cu2–O22	83.7 (3)
O3–Gd–O4	66.7 (2)	O21–Cu2–O22	96.3 (3)
O3–Gd–O5	68.7 (2)	O21–Cu2–O23	89.5 (7)
O3–Gd–O6	134.2 (2)	O21–Cu2–O23	90.5 (7)
O3–Gd–O7	147.6 (2)	O21–Cu2–O22	96.3 (3)
O3–Gd–O8	128.9 (2)	O21–Cu2–O22	83.7 (3)
O3–Gd–O9	76.1 (2)	O21–Cu2–O23	90.5 (7)
O4–Gd–O5	71.1 (2)	O21–Cu2–O23	89.5 (7)
O4–Gd–O6	91.8 (2)	O22–Cu2–O22	180.(0)
O4–Gd–O7	135.5 (2)	O22–Cu2–O23	92.1 (8)
O4–Gd–O8	69.2 (2)	O22–Cu2–O23	87.9 (8)
O4–Gd–O9	78.1 (2)	O23–Cu2–O23	180.(2)
O5–Gd–O6	66.1 (2)	Gd–Gd–Cu1	109.98 (1)
O5–Gd–O7	134.3 (2)	Gd–Gd–Cu2	111.62 (0)
O5–Gd–O8	118.5 (2)	Cu1–Gd–Cu1	135.91 (1)
O5–Gd–O9	140.0 (2)	Cu1–Gd–Cu2	81.41 (1)
O6–Gd–O7	75.5 (2)	Gd–Cu1–Gd	171.67 (3)
O6–Gd–O8	70.3 (2)	Gd–Cu2–Gd	180.00 (0)
O6–Gd–O9	140.9 (2)		

[a] Numbers in parentheses are estimated standard deviations in the least significant digits.

direction is identified and shown in Figure 1a. The ladders are not isolated from each other; rather, they are associated across oxalato groups, which act as bridges between Gd(III) ions along the monoclinic *b*-axis direction. The oxalato bridges promote a remarkable two-dimensional pattern of association of the ladders. This is evidenced by the observation of a double-sheet thick honeycomb network based on distorted hexagonal rings, as shown in Figure 1b. These rings are not regular since two opposite edges are Gd(ox)Gd sequences with a Gd···Gd separation of 6.336 (1) Å, while the other four edges are linear Gd[Cu(pba)]Gd sequences with average Gd···Gd and Gd···Cu separations of 11.431 (1) and 5.716 (1) Å, respectively. Specifically, the Gd···Gd separations through the Cu(pba) bridge range from 11.402 (1) to 11.460 (1) Å, while the Gd···Cu separations across the oxamato bridge vary from 5.693 (1) to 5.739 (1) Å. Note that the formation of such rings is reminiscent of the linkage of La(III) ions by oxalato groups, which form similar, albeit regular, hexagonal rings inside infinite single layers, as demonstrated recently in the structure of $La_2(ox)_3(H_2O)_{9.5}$.[12,13] The Gd(III) ions adopt a distorted

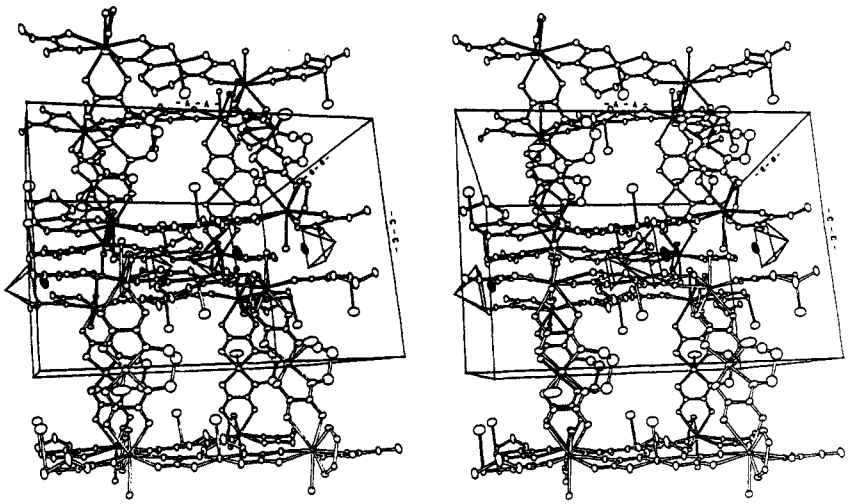

Figure 3. Stereoscopic view along *b*, down the gap between the slabs.

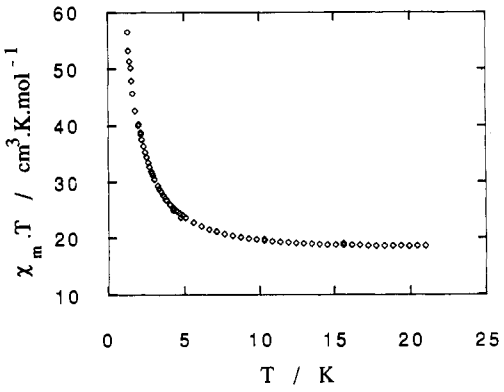

Figure 4. $\chi_M T$ versus T plot in the 20–1.3 K temperature range.

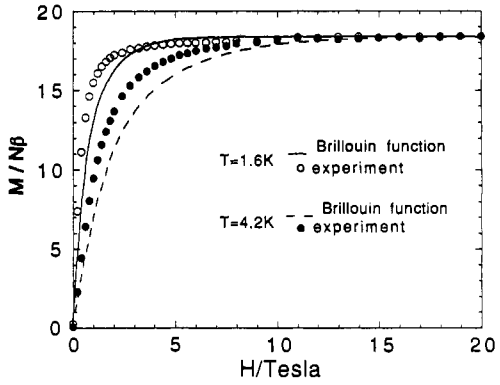

Figure 5. Magnetization M versus magnetic field H curves at 1.6 and 4.2 K.

capped square antiprism coordination of oxygen atoms (Figure 2). Six out of a total of nine oxygen atoms are provided by the three bridging Cu(pba) groups, two by the oxalato ligand, and the last one by a water molecule. The Cu(II) ions of the Cu(pba) units present a classical square-pyramidal environment with a water molecule in the apical position. Additional Cu(II) ions are found in discrete, hydrogen-bonded square-pyramidal $[Cu(H_2O)_5]^{2+}$ units, interspersed in the gap between the layers. Those charged species might serve to anchor the slabs to each other along the transverse *c* axis direction, as exemplified in Figure 3 where one looks down the gap in a direction parallel to the *b* axis. Note also that these units were located very close to the mirror planes and were subsequently disordered in the structure; one orientation only is depicted in Figure 3.

Magnetic Properties

We will present successively the zero-field magnetic susceptibility and the low- and high-field magnetizations. The $\chi_M T$ versus T plot for **1** is shown in Figure 4. χ_M is the molar magnetic susceptibility, and T, the temperature. At room temperature, $\chi_M T$ is equal to 17.2 cm^3 K mol^{-1}. This value corresponds to that expected for two Gd(III) and four Cu(II) noninteracting magnetic centers with the local g factors $g_{Gd} = g_{Cu} = 2.0$. Indeed, $\chi_M T$ is then given by $(N\beta^2/k)(21g_{Gd}^2/2 + g_{Cu}^2)$, where N is the Avogadro number, β the Bohr magnetron, and k the Boltzmann constant. When the temperature is lowered, $\chi_M T$ remains essentially constant down to ca. 30 K and then increases more and more rapidly and reaches 60 cm^3 K mol^{-1} at 1.3 K. This behavior unambiguously indicates that the $S_{Gd} = {}^7/_2$ local spins tend to align along the same direction. Those data, however, do not specify whether the $S_{Cu} = {}^1/_2$ local spins of the Cu(pba) groups align along the same direction (ferromagnetic behavior) or along the opposite direction (ferrimagnetic behavior). In the 2–20 K temperature range, these magnetic susceptibility data could be described by a Curie–Weiss law $\chi_M = C/(T-\Theta)$ with a Weiss constant Θ = 1.25 (3) K.

The dependence of the magnetization M as a function of the field H was investigated at various temperatures below 5 K both in the low-field regime with the SQUID magnetometer (below 200 G) and in the high-field regime at the "Service des Champs Intenses" (up to 20 T). In the low-field regime and at any temperature, the M versus H plot is linear, with a slope in perfect agreement with the zero-field susceptibility value measured independently. Those low-field experiments do not show any indication of spin decoupling, i.e. an increase of the slope dM/dH above a certain value of the field. The experimental data in the high-field regime at 1.6 and 4.2 K are shown in Figure 5 together with the theoretical curves for two Gd(III) and four Cu(II) noncoupled ions, i.e. Brillouin's functions. At both temperatures the magnetization increases faster than expected for noninteracting ions. The saturation magnetization M_S is equal to $18N\beta$, which exactly corresponds to the value anticipated for all the local spins aligned along the same direction ($M_S = 2g_{Gd}S_{Gd} + 4g_{Cu}S_{Cu}$). One recalls that $N\beta$ = 5583 cm^3 G mol^{-1}.

Discussion

The zero-field magnetic susceptibility data down to 1.3 K clearly reveal that the S_{Gd} local spins tend to align along the same direction but do not allow one to specify if the Gd(III)–Cu(II) interaction through the oxamato bridge is antiferro- or ferromagnetic. Those susceptibility data also indicate that the three-dimensional ordering, if any, should occur below 1.3 K, the lowest temperature we can reach with our instruments.

Additional information may be gained by an analysis of the magnetization measurements. Before interpreting the experimental data, let us sum up the various situations we could en-

(12) Ollendorff, W.; Weigel, F. *Inorg. Nucl. Chem. Lett.* **1969**, *5*, 263.
(13) Michaelides, A.; Skoulika, S.; Aubry, A. *Mater. Res. Bull.* **1988**, *23*, 579.

counter according to the nature and the magnitude of the Gd(III)–Cu(II) interaction. Since the $[Cu(H_2O)_5]^{2+}$ units are interspersed in the gap between the double-sheet layers, we assume that the interaction between those units and the polymeric skeleton, if any, is very weak. Magnetic interaction may occur through hydrogen bonds;[14-16] however, in the present case, the $[Cu(H_2O)_5]^{2+}$ units are shielded by the network of noncoordinated water molecules. Thus, the measured magnetization may be approximated by the sum of two contributions, one due to the two-dimensional network $\{Gd_2(ox)[Cu(pba)]_3\}^{2-}$, the other one due to the discrete $[Cu(H_2O)_5]^{2+}$ unit:

$$M = M(\text{network}) + M(\text{isolated } Cu^{2+})$$

(i) If the magnetic centers were all noncoupled, M (in $N\beta$ units) would vary according to

$$M = 2g_{Gd}S_{Gd}B_{7/2}(y_{Gd}) + 4g_{Cu}S_{Cu}B_{1/2}(y_{Cu})$$

where $B_{7/2}(y_{Gd})$ and $B_{1/2}(y_{Cu})$ are the Brillouin functions for the Gd(III) and Cu(II) ions, respectively. This M variation hereafter is referred as the Brillouin curve. The saturation magnetization would be given by

$$M_S = 2g_{Gd}S_{Gd} + 4g_{Cu}S_{Cu}$$

i.e. equal to $18N\beta$.

(ii) If the Gd(III) and Cu(II) ions within the two-dimensional network were strongly coupled antiferromagnetically, the magnetization would at first increase faster than the Brillouin curve, since the zero-field susceptibility is larger in the ferrimagnetic case than in the paramagnetic one, and then would reach a saturation given by

$$M_S = 2g_{Gd}S_{Gd} - 2g_{Cu}S_{Cu}$$

i.e. equal to $12N\beta$. It follows the M versus H curve would intersect the Brillouin curve.

(iii) If the interaction between Gd(III) and Cu(II) ions through the oxamato bridge was weakly antiferromagnetic, then the field could decouple the S_{Gd} and S_{Cu} spins. If so, the magnetization curve instead of showing a continuous increase and then a saturation would vary as follows: First, M would increase faster than the Brillouin curve and then would reach an intermediate plateau with a magnetization close to $12N\beta$; the lower the temperature would be, the more pronounced this plateau. When the field is further increased, the second derivative d^2M/dH^2 would change sign for a field value corresponding to the crossover between the antiparallel and parallel spin states. Such a crossover for weakly antiferromagnetically coupled compounds has recently been reported.[17,18] Finally, the magnetization would increase from the ferrimagnetic saturation ($12N\beta$) up to the ferromagnetic one ($18N\beta$), the M variation being now slower than the Brillouin curve, since the antiferromagnetic interaction opposes the field. It follows that the experimental magnetization curve would also intersect the Brillouin curve.

The experimental curves are not as expected for (i)–(iii). No plateau is observed, even at low field. The slope dM/dH of the M versus H plot first is constant, then progressively diminishes, and finally tends to zero when a saturation of $18N\beta$ is reached. In the whole field range, the M versus H curve is above the Brillouin curve. Therefore, the Gd(III)–Cu(II) interaction through the bisbidentate bridge is actually ferromagnetic. Even in zero field, the S_{Gd} and S_{Cu} local spins tend to align along the same direction.

We have checked by studying the magnetic properties of $Gd_2(ox)_3(H_2O)_{9.5}$ containing also Gd(ox)Gd linkages[12,13] that the Gd(III)–Gd(III) interaction through the oxalato bridge is very weakly antiferromagnetic. If this Gd(III)–Gd(III) interaction is neglected, the structure to be considered is that of infinite ladders in which all the exchange pathways between nearest neighbors are identical, schematized as follows:

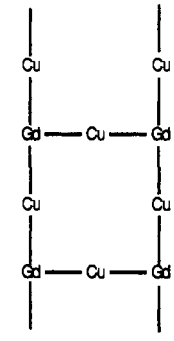

There is no available model to fit the magnetic data for such a system yet, even in the approximation where S_{Gd} is treated as a classical spin. A very rough estimate of the J interaction parameter ($H = -JS_{Gd}S_{Cu}$) may be deduced from the Weiss constant Θ in the mean-field approximation, which leads to $J = 0.15$ cm^{-1}. De Jongh and Miedema have pointed out the deficiency of the mean-field approximation for low-dimensional systems[19] so that this J value may be considered at the best as accurate to one order of magnitude. The ferromagnetic nature of the Gd(III)–Cu(II) interaction confirms the results of Gatteschi et al.[20,21] and Okawa et al.,[22] who characterized Gd(III)–Cu(II) ferromagnetic interactions in di- and trinuclear species. In our case, however, the interaction occurs in spite of the large separation between the magnetic centers. Furthermore, the effect of the Gd(III)···Cu(II) ferromagnetic interaction is enhanced, since **1** is a two-dimensional material and not a loose assembly of isolated molecular units.

Much work remains to do concerning this new class of molecular materials associating rare earths and 3d metal ions within a polymeric network and containing discrete units intercalated between the slabs. We anticipate that quite interesting magnetic and optical properties will be observed.

Supplementary Material Available: Structure determination details (Table SI), anisotropic thermal parameters (Table SII), and bond lengths and angles (Table SIII) (6 pages); a listing of structure factors (24 pages). Ordering information is given on any current masthead page.

(14) Culvahouse, J. W.; Francis, C. L. *J. Chem. Phys.* **1977**, *66*, 1079.
(15) Bertrand, J. A.; Helm, F. T. *J. Am. Chem. Soc.* **1973**, *95*, 8184. Bertrand, J. A.; Black, T. D.; Eller, P. G.; Mahmood, R. *Inorg. Chem.* **1976**, *15*, 2965.
(16) Hendrickson, D. N. In *Magneto-Structural Correlations in Exchange Coupled Systems*; Willet, R. D., Gatteschi, D., Kahn, O., Eds.; NATO ASI Series; Reidel: Dordrecht, The Netherlands, 1985.
(17) Qiang, X.; Darriet, J. C. *C. R. Acad. Sci. Paris* **1988**, *303*, 1637.
(18) Menage, S.; Vitols, S. E.; Bergerat, P.; Codjovi, E.; Kahn, O.; Girerd, J. J.; Guillot, M.; Solanz, X.; Calvet, T. *Inorg. Chem.* **1991**, *30*, 2666.
(19) De Jongh, L. J.; Miedema, A. R. *Adv. Phys.* **1974**, *23*, 1.
(20) Bencini, A.; Benelli, C.; Caneschi, A.; Carlin, R. L.; Dei, A.; Gatteschi, D. *J. Am. Chem. Soc.* **1985**, *107*, 8128.
(21) Benelli, C.; Caneschi, A.; Gatteschi, D.; Guillou, O.; Pardi, L. *Inorg. Chem.* **1990**, *29*, 1750.
(22) Matsumoto, N.; Sakamoto, M.; Tamaki, H.; Okawa, H.; Kida, S. *Chem. Lett.* **1989**, 853.